

(12)

DA025953

IR OPTICAL WAVE GUIDES

J. S. Haggerty and W. L. Robbins
ARTHUR D. LITTLE, INC.
Cambridge, Massachusetts 02140

MAY 1976

FINAL REPORT

Sponsored by
Advanced Research Projects Agency
ARPA Order No. 2327

The views and conclusions contained in this document are those of the authors and should not be interpreted as necessarily representing the official policies, either expressed or implied, of the Advanced Research Projects Agency or the U.S. Government.

Prepared under Contract No. N00014-73-C-0263

for
DEPARTMENT OF THE NAVY
OFFICE OF NAVAL RESEARCH
ARLINGTON, VA 22217

DDC
RECEIVED
JUN 24 1976
RECEIVED

DISTRIBUTION STATEMENT A
Approved for public release

ADA025953

UNCLASSIFIED

SECURITY CLASSIFICATION OF THIS PAGE (When Data Entered)

REPORT DOCUMENTATION PAGE		READ INSTRUCTIONS BEFORE COMPLETING FORM
1. REPORT NUMBER	2. GOVT ACCESSION NO.	3. RECIPIENT'S CATALOG NUMBER
4. TITLE (and Subtitle)		5. TYPE OF REPORT & PERIOD COVERED
6 IR Optical Wave Guide	9	Final Report. Feb 73 - May '76
7. AUTHOR(s)		6. PERFORMING ORG. REPORT NUMBER
10 J. S. Haggerty W. L. Robbins	15	
9. PERFORMING ORGANIZATION NAME AND ADDRESS		8. CONTRACT OR GRANT NUMBER(s)
Arthur D. Little, Inc. Cambridge, Massachusetts 02140		N00014-73-C-0263
11. CONTROLLING OFFICE NAME AND ADDRESS		10. PROGRAM ELEMENT, PROJECT, TASK AREA & WORK UNIT NUMBERS
Department of the Navy Office of Naval Research Arlington, Virginia 22217	11	ARPA Order N00-2327
14. MONITORING AGENCY NAME & ADDRESS (if different from Controlling Office)		12. REPORT DATE
12 HRP		May 1976
		13. NUMBER OF PAGES
		39
		15. SECURITY CLASS. (of this report)
		Unclassified
		15a. DECLASSIFICATION/DOWNGRADING SCHEDULE
		N/A
16. DISTRIBUTION STATEMENT (of this Report)		
Reproduction in whole or in part is permitted for any purpose of the U.S. Government.		
17. DISTRIBUTION STATEMENT (of the abstract entered in Block 20, if different from Block 16)		DISTRIBUTION STATEMENT A Approved for public release; Distribution Unlimited
ONR Scientific Officer: T. G. Giallorenzi, Code 5500 tel.: (202) 767-2499		
Amount of Contract: \$118,300.00		
18. SUPPLEMENTARY NOTES		
This research was supported by the Advanced Research Projects Agency of the Department of Defense and was monitored by ONR under Contract No. N00014-73-C-0263.		
19. KEY WORDS (Continue on reverse side if necessary and identify by block number)		
Optical Wave Guides Glass Fiber Drawing		
20. ABSTRACT (Continue on reverse side if necessary and identify by block number)		
Techniques are described by which As_2Se_3 glass fibers were drawn and characterized. The fibers were designed to transmit a single or at most a few optical modes of 10.6 μm radiation. The fibers were characterized optically and physically. Optical characterization included measure- ment of optical absorption coefficient. micrometers continued -		

DD FORM 1473
1 JAN 73

UNCLASSIFIED

SECURITY CLASSIFICATION OF THIS PAGE (When Data Entered)

UNCLASSIFIED

SECURITY CLASSIFICATION OF THIS PAGE (When Data Entered)

20.

The drawing process was found well controlled and functioned according to glass drawing theory. The optical absorption coefficient was adversely effected by the materials handling procedures which were utilized; however, it was demonstrated that low loss fibers can be drawn by this process. Further work is required to identify the nature of the dominant absorption coefficient and its origin in the fiber drawing process.

ACCESSION for	
HTIS	White Section <input checked="" type="checkbox"/>
RCC	Buff Section <input type="checkbox"/>
EXAM/CO-CEN	<input type="checkbox"/>
IDENTIFICATION	
<i>Per Hx. on file</i>	
BY	
DISTRIBUTION/AVAILABILITY CODES	
Dist.	AVAIL. and/or SPECIAL
<i>A</i>	

DDC
RECEIVED
JUN 24 1976
D

UNCLASSIFIED

SECURITY CLASSIFICATION OF THIS PAGE (When Data Entered)

TABLE OF CONTENTS

	<u>Page</u>
I. Introduction	I-1
II. Fiber Design Characteristics	II-1
A. General Fiber Design Parameters	II-1
B. Materials Selection	II-2
III. Fiber Drawing	III-1
A. Concentric-Orifice Fiber-Drawing Apparatus	III-1
1. Design Criteria	III-1
2. Experimental Apparatus	III-2
a. Orifice Reservoir System	III-2
b. Furnace	III-4
c. Fiber Drawing Collet	III-5
B. Fiber Pulling Experiments	III-5
1. Feed Material Selection	III-5
2. Feed Preparation	III-6
3. Fiber Drawing	III-7
4. Analysis of Fiber Drawing Process	III-11
IV. Optical Characterization	IV-1
A. Sample Preparation	IV-1
B. Apparatus for Optical Attenuation Measurements	IV-1
C. Attenuation Coefficient	IV-3
D. Results of Optical Attenuation Measurements	IV-4
V. Conclusions	V-1
VI. References	VI-1

LIST OF FIGURES

	<u>Page</u>
1. Refractive Index as a Function of Composition for the System $As_2Se_3 - As_2Te_3$	II-5
2. Schematic Representation of Furnace and Double Orifice Assembly	III-3
3. Kinematic Viscosity of As_2Se_3 Glass as a Function of Temperature	III-12
4. Fiber Diameter Vs. Pulling Speed	III-13
5. Schematic Representation of Apparatus Utilized for Optical Attenuation and Numerical Aperture Measurements	IV-2
6. Representative Relative Transmission Measurements. Fiber Designations and Calculated Absorption Coefficients are Shown	IV-5
7. Normalized Relative Transmission ($T_{R,G}$) as a Function of Annular Cone Angle	IV-8

LIST OF TABLES

	<u>Page</u>
1. Summary of Drawing Conditions and Physical Characteristics of As_2Se_3 Glass Fibers	III-9
2. Summary of Glass Process History	III-10

I. INTRODUCTION

There has been a growing interest in optical waveguides for a wide variety of applications dealing with information transmission. This has been particularly true for light wave lengths near $1.0 \mu\text{m}$ where emitter, transmission-cable and detector technologies have all developed viable solutions more or less simultaneously. Prior to this program, there had been essentially no work on developing long wavelength infrared optical fibers--primarily because clearly defined applications had not been identified where they could be used to advantage. In response to emerging applications, we have developed procedures for drawing optical fibers designed to transmit a single mode of $10.6 \mu\text{m}$ light as well as multiple modes over a range of wavelengths from approximately 1 to beyond $15 \mu\text{m}$.

The possibility of radar systems based on high power CO_2 lasers, which emit at $10.6 \mu\text{m}$, was the prime reason for developing fiber pulling procedures applicable to materials which transmit at $10.6 \mu\text{m}$. Other applications for IR fibers have become apparent which are probably more achievable. The resolution of images processed by detector arrays can be improved by focusing an image onto a bundle of fibers which in turn transmit the light to remote detectors rather than focusing directly on the detector array. Infrared optical systems can be simplified by using fiber plates to transform images from arbitrarily curved focal surfaces to planar focal surfaces. Gimbaled, optical guidance control systems, used in certain missiles, can be simplified by utilizing IR fiber optics. Other applications include face plates for long wavelength IR image intensifiers and waveguides for transmitting signals into and out of dewars to cooled emitters or detectors. We believe that many applications for IR fiber optics have remained dormant because the fibers have not been generally available to optical engineers.

The objective of this experimental program has been to develop techniques by which fibers can be drawn which will transmit a single or at most a few optical modes of $10.6 \mu\text{m}$ light. Achieving extremely low optical attenuation coefficients was not a main goal. Whenever possible, core and cladding materials were selected from those which were commercially

available and had been thoroughly characterized. Representative fibers were supplied to the contract officer.

Earlier in this program, 10.6 μm optical wave guides were produced in the form of single crystal germanium fibers. Initially, it was decided to limit candidate materials to single crystals because it was felt that optical quality single crystal fibers could be produced sooner than glass fibers. The results of this phase of work, which was based on the ADL-CO₂ laser heated fiber growth process, was reported in June, 1974. The readers are referred to previous reports for complete descriptions of the single crystal fiber growth process and our work with germanium. In the phase of work described in this report, we concentrated on chalcogenide glass fibers.

II. FIBER DESIGN CHARACTERISTICS

A. General Fiber Design Parameters

Suitable fibers must satisfy several criteria simultaneously. The core and cladding refractive indices and core diameters must be matched so the number of transmitted modes will be limited either to a single mode, or at most, a few modes. The core diameter should be maximized to facilitate optical coupling as well as reducing the effect of microstructural defects on attenuation of the transmitted light. The cladding thickness must be large enough to eliminate leakage losses of the evanescent wave. We did not attempt to produce minimum acceptable thickness claddings since fiber packing density in bundles was not considered important at this time. However, the overall fiber diameter is limited by stresses induced during normal fiber flexure.

Cylindrical dielectric waveguides with step-refractive index variations are characterized by the following expression:⁽¹⁾

$$V = \frac{\pi d}{\lambda_0} (2\bar{n}\Delta n)^{1/2}$$

where d = core diameter

λ_0 = free space light wavelength

\bar{n} = average refractive index of core and cladding

Δn = the difference between core and cladding refractive indices

Below $V \approx 2.4$, the fibers propagate a single mode, designated HE_{11} . For $V \gg 2.4$ the quantity of propagating modes (N) is⁽³⁾

$$N \approx \frac{V^2}{2}$$

For V 's slightly greater than 2.4, one must determine which specific low order modes are transmitted. One additional mode, the first order transverse electric wave mode (TE_{01}), is allowed for $2.4 < V < 5.5$.⁽⁴⁾ The clad fibers grown in this program were designed to make V as close to 2.4 as practical; thus maximizing the core diameter without allowing many modes to propagate.

The core diameter is also maximized, for a given V , by minimizing the Δn between the core and cladding. The minimum Δn that can be considered practical with glasses is approximately 0.005 because of compositional variations and residual stresses induced during pulling.⁽³⁾ Thus, the core diameter for a typical single mode chalcogenide glass fiber ($n = 2.7$) must be smaller than approximately 50 μm .

The minimum cladding thickness is determined by the maximum acceptable leakage between fibers as well as by the requirement to be thick enough to carry the fraction of the signal transmitted in the cladding. The power density of the evanescent wave decreases exponentially with distance from the core-cladding interface. In general, a cladding thickness of one to two wavelengths is large enough to reduce the light transmitted into a third medium (leakage) to less than 0.001% per reflection.⁽⁴⁾ The fibers produced during this program had cladding thicknesses of the order of 10-12 wavelengths so that leakage should be negligible.

Overall fiber diameters were generally limited to less than 150 μm so the fibers could be flexed without breaking. Based on properties of typical chalcogenide glasses, the 150 μm diameter fibers can be bent to an 18 cm radius of curvature without inducing tensile stresses in excess of 6.89×10^7 dyne/cm² (1000 psi). Fibers of this diameter can be subjected to smaller radii of curvature without breaking; however, this figure represents a reasonable design limit.

B. Materials Selection

The constituent materials used for these optical wave guides should meet the following criteria: (1) have low optical absorptivities for 10.6 μm radiation, (2) exist as core and cladding materials combinations which simultaneously satisfy refractive index, chemical compatibility and processing requirements, (3) be amenable to drawing to appropriate core diameters, (4) withstand reasonable service environments, and (5) permit the core diameters to be measured while imbedded in claddings.

The single crystal Ge fibers, which were reported previously, met most, but not all, of these criteria. The single crystal growth process did not permit growing fibers less than 25 μm in diameter without extensive modification of the optical components in the laser-heated fiber

growth apparatus. Thus, with all potentially suitable cladding materials that were identified, the Ge-core fibers would have been multimode because core diameters were too large.

Unlike crystalline semiconductors, refractive indices of glasses can be easily adjusted with compositional changes without effecting the optical absorptivity or the growth process. Most additions to semiconductors result either in free carrier absorption or adversely effect the growth process because of low distribution coefficients. Glass fibers can be produced with better surface finishes than single crystal fibers since faceting persists to some extent in all single crystals--causing at least a noncircular cross section and often surface roughness. Glass fibers can be clad during the drawing process, which preserves the quality of the as-drawn surfaces. We found no cladding process, other than post growth processes, for single crystal fibers. Thus, glass fibers have several distinct advantages over single crystal fibers provided low optical absorptivities can be attained.

At the beginning of the program single crystals had exhibited substantially lower bulk absorptivities to 10.6 μm light than glasses. Recently, Maklad, et al⁽⁵⁾ reported 10.6 μm absorptivities in the range of 10^{-2} cm^{-1} for As_2Se_3 which was low enough for the objectives of this program. As_2Se_3 glass also appeared to satisfy the other criteria for an acceptable optical fiber. Other than a few modeling experiments with As_2S_3 , all of the fibers grown during this program were based on As_2Se_3 host glasses.

In addition to a low optical absorptivity for 10.6 μm light, As_2Se_3 satisfied the other criteria for an optical fiber. At fiber drawing temperatures ($\sim 310\text{-}320^\circ\text{C}$), the vapor pressure is low enough that no special techniques are required to suppress vaporization. The host and doped glasses are stable with respect to devitrification and apparently show no tendency to phase separate. These glasses are reasonably inert--they are not attacked by moisture or organic solvents. Finally the refractive index can be adjusted without affecting the thermal expansion coefficient or viscosity characteristics significantly.

The As_2Se_3 refractive index can be adjusted either by changing the As/Se ratio⁽⁶⁾ or with additions such as Te.⁽⁷⁾ Either approach appears equally suitable from performance criteria. We chose to raise the core glass index with a Te addition so that the core diameter could be measured by an X-ray probe technique.

The refractive indices for mixed $\text{As}_2\text{Se}_3 - \text{As}_2\text{Te}_3$ glasses, as determined by reflectivity experiments, are given in Figure 1.⁽⁷⁾ The index rises at an initial rate $\frac{dn}{dx} = 0.939$ for small As_2Te_3 additions. For example, a $\Delta n \approx 0.02$ results from approximately a 2.2% As_2Te_3 substitution. This rate of index change results in a doping level which can be mixed homogeneously and which can be detected by the X-ray probe technique.

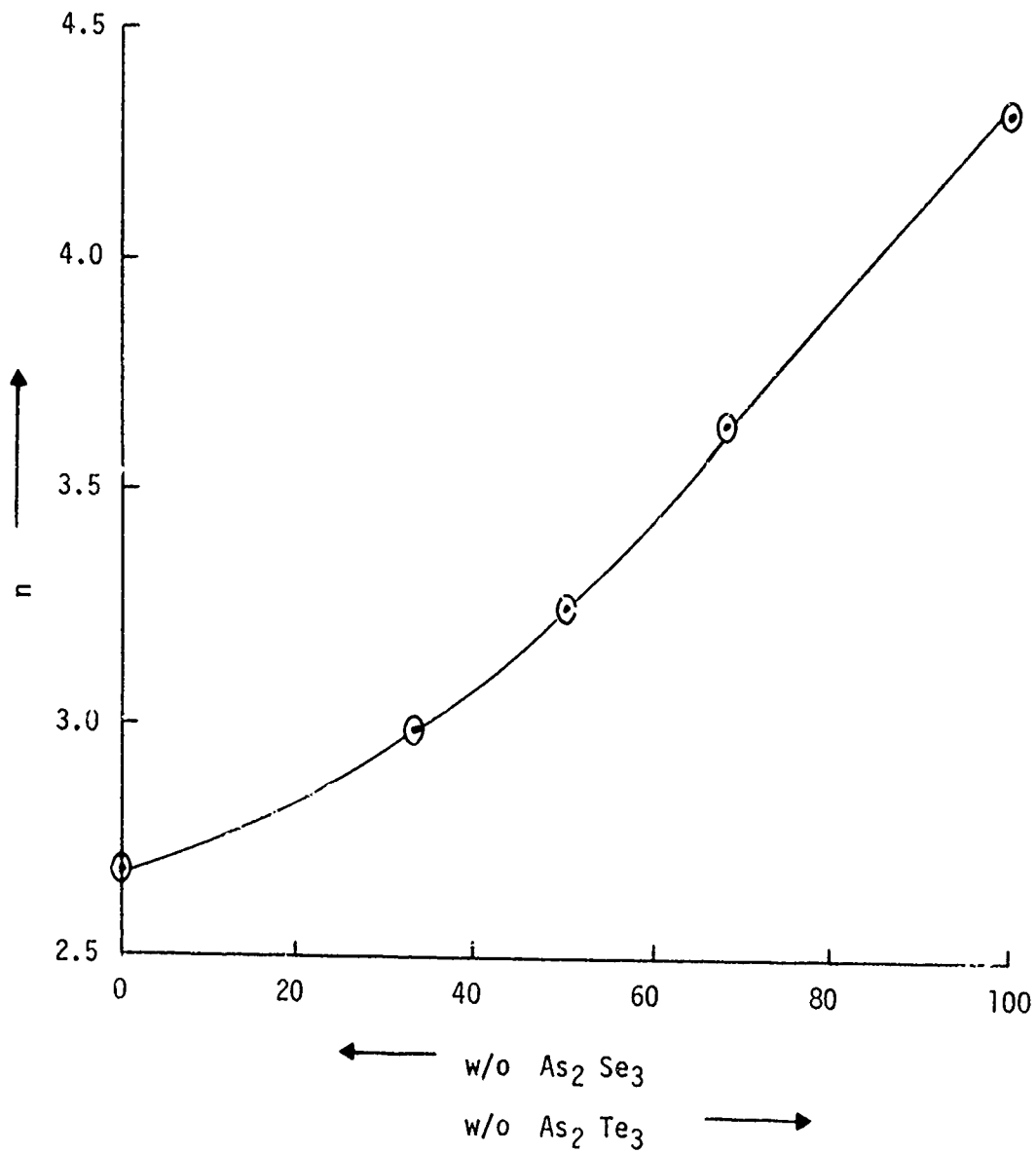


FIGURE 1 REFRACTIVE INDEX AS A FUNCTION OF COMPOSITION FOR THE SYSTEM
 $As_2Se_3 - As_2Te_3$

III. FIBER DRAWING

A. Concentric-Orifice Fiber-Drawing Apparatus

1. Design Criteria

A concentric orifice fiber-growth bushing functions in a manner which is similar to a single orifice bushing except that the core and cladding are drawn simultaneously. The core glass is drawn through an inner orifice from one reservoir of glass and the cladding is drawn through a surrounding orifice from a separate reservoir of glass. The glass flow rates through the two orifices are determined by the hydrostatic heads of the glasses above the orifices, the viscosities of the glasses, the orifice lengths, and the orifice areas. The core and cladding glass flow rates are independently controlled by adjusting one or more of these parameters, and by so doing, the area ratios of the two regions in the drawn fiber are established since there is no convective or diffusion mixing between the two. The overall diameter of the drawn fiber is controlled by the pulling velocity by the equality between the total mass flow rate through the concentric orifices with that withdrawn in the fiber. The thermo-physical properties of the core and cladding glasses should be matched as closely as possible. High residual stresses result from differences between viscosities, thermal expansion coefficients and set points.

The mass flow rate through a single orifice is described by Poiseuille's equation as follows:⁽⁸⁾

$$F \propto \frac{r^4 h}{\ell \eta}$$

where F = flow rate (gm/hr)
 r = orifice internal radius (cm)
 h = head of glass above orifice (cm)
 ℓ = orifice length (cm)
 η = glass viscosity (Poise)

The proportionality constant was determined by analyzing data for conventional single orifice glass drawing processes. This yielded:

$$F = \frac{1.8 \times 10^6 r^4 h}{\ell \eta}$$

The specific dimensions of the concentric orifice and reservoirs were developed using the following criteria. The cross sectional areas of the inner and outer orifices were scaled to produce relative flow rates corresponding to the desired core/cladding diameter ratios. Similarly, the cross sectional areas of the reservoirs were made equivalent to the desired diameter ratios so the relative heads of glasses in the two reservoirs would not change during a fiber drawing run. The initial heads and cross sectional areas of the reservoirs were selected so that hydrostatic heads would not vary more than 10% during a fiber drawing run corresponding to a 100 meter long, 150 μm diameter fiber. The orifice diameters were determined based on 10 cm/sec pulling rates with glass viscosities equal to 1000 Poise. The area of the exterior orifice was made adjustable so the relative core and cladding glass flow rates could be adjusted to conform to the desired values. These features are reflected in the concentric orifice fiber pulling apparatus described in the following section.

2. Experimental Apparatus

a. Orifice Reservoir System

The concentric orifice-reservoir system which was used in these fiber pulling runs is shown schematically in Figure 2. Fused silica glass tubing was used for both elements of the assembly.

The internal and external diameters of the inner reservoir were 0.41 and 0.59 cm respectively. The internal diameter of the exterior reservoir was 1.6 cm. These give an Area-Core/Area-Cladding ratio for the reservoirs equal to 0.0759 which corresponds to a 40 μm diameter core in a 150 μm diameter fiber.

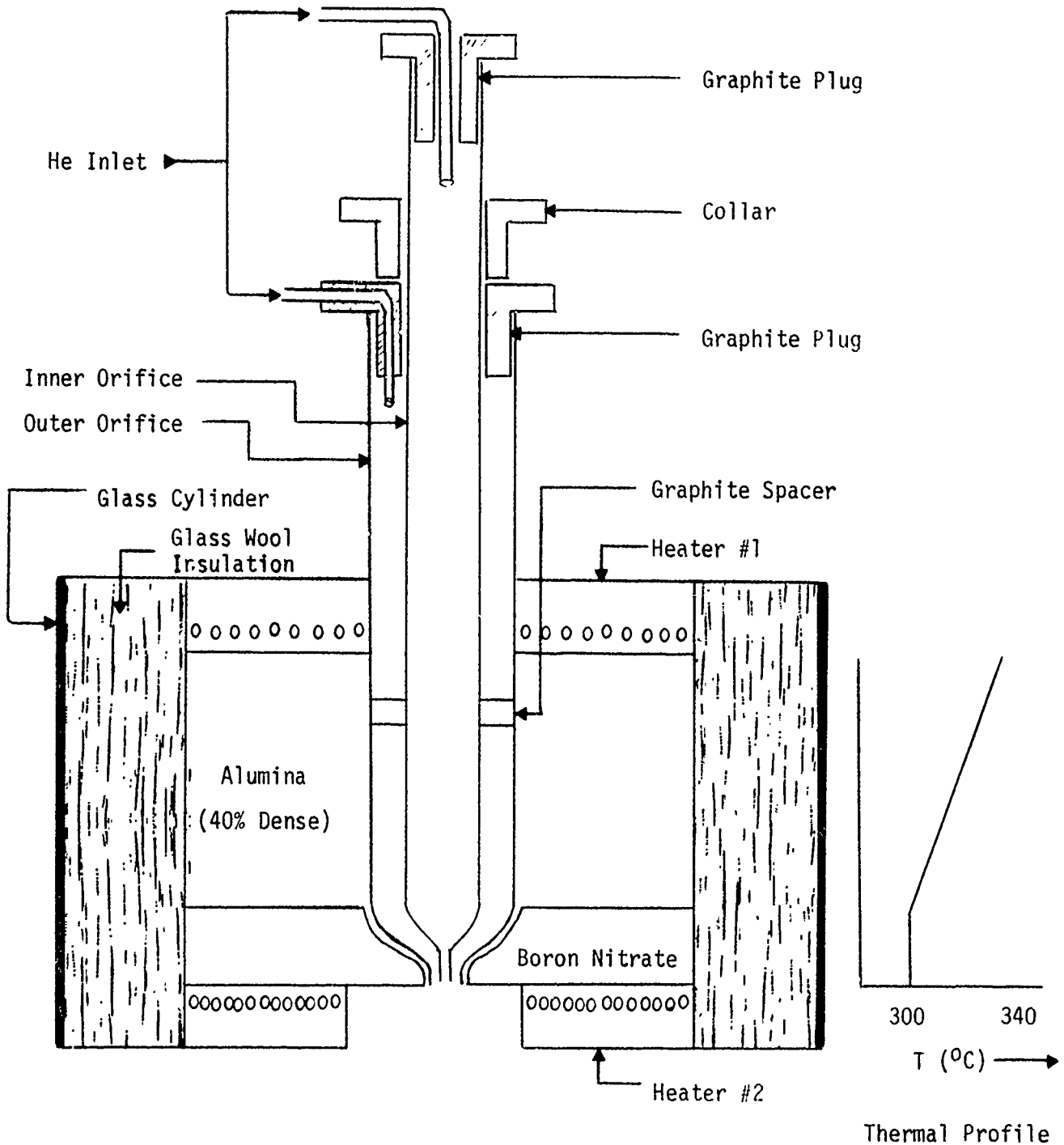


FIGURE 2 SCHEMATIC REPRESENTATION OF FURNACE AND DOUBLE ORIFICE ASSEMBLY

The tips were formed by working the quartz tubing and grinding them to give ends which were smooth and perpendicular to the tube axes. The inner tip was approximately 0.12 cm internal diameter and 0.71 cm long. The external tip was approximately 0.34 cm internal diameter and 0.1 cm long. Correct relative core and cladding glass flow rates could be achieved with these orifice dimensions.

The cladding glass orifice area was adjusted by changing the relative positions of the inner and external tubes. Reference measurements were made between the ends of the two tips. The collar, shown in Figure 2, was used to maintain a relative position between the tubes once it was established.

Concentricity between the inner and exterior tubes was maintained by means of high purity graphite spacers. This design feature permitted the components to be assembled to reproducible dimensions after cleaning as well as maintaining alignment when internal and external tubes were moved relative to one another while adjusting the exterior orifice area.

Both of the tubes were capped with high purity graphite plugs through which helium was introduced when the glasses were hot. The flowing gas provided a protective atmosphere, thereby avoiding oxygen contamination. Oxygen contamination in the tip area during drawing did not present a problem because of short exposure times.

This orifice-reservoir proved quite easy to fill with feed glasses and to pull correct dimension fibers from. We experienced no breakage of the fused silica tips and reservoirs due to mismatches in thermal expansion coefficients.

b. Furnace

The furnace used to heat the glass in the orifice-reservoir system is also shown schematically in Figure 2. It was designed to produce a uniform temperature in the orifice region and a linearly increasing temperature upward through the reservoir region. The latter feature prevents convection in the glasses; thus, the fibers are pulled from quiet liquids.

The desired temperature profile was achieved by means of inducing axial heat flow through two materials with dissimilar thermal conductivities. Upper and lower heaters established the temperature throughout the reservoir region: the temperature in the orifice region was set by the lower heater and distributed by the relatively high thermal conductivity BN plate. A linear temperature gradient through the Al_2O_3 which surrounded the reservoirs was established by radially insulating the intermediate thermal conductivity Al_2O_3 .

The heater plates were constructed by imbedding helically wound resistance wire into alumina cement. Temperatures were monitored by means of thermocouples imbedded in each heater plate. Each heater plate temperature level was independently controlled.

This relatively simple furnace design achieved the desired temperature profile and proved reliable in operation.

c. Fiber Drawing Collet

A simple collet (fiber spooling mechanism) was constructed for this program. It consisted of a variable speed, nontraversing paper faced drum. The drum diameter was 16.9 cm. It was driven by means of a variable speed d.c. motor at surface rates ranging from 160 to 1460 cm/sec. Timing belt drives were utilized to prevent slippage.

Surface velocities were measured directly by means of wheel driven instrumentation for purposes of calibration and determining the uniformity of pulling speeds. Preset pulling speeds were constant within 2%.

A traversing feature was not required on this collet because pulled fiber lengths were generally less than 100 meters. With 150 μ m diameter fibers, this fiber length occupied less than 3 cm of drum length. No problems were experienced with fibers crossing over previously wound turns.

B. FIBER PULLING EXPERIMENTS

1. Feed Material Selection

Several sources of feed materials for the As_2Se_3 fibers were surveyed. It was felt preferable to work with commercially available

materials if possible since materials synthesis, homogenization and purification consistent with the requirements of this program would be disproportionately time consuming. Small quantities of experimental materials were made available by several sources but their use was not considered appropriate because the future supply of identical materials could not be insured. Most of our work was done with As_2Se_3 samples purchased from Cerac, Inc. of Butler, Wisconsin and Unimetrics Corporation of Anaheim, California.

The material purchased from Cerac were 5 9's pure As_2Se_3 sputtering disks. X-ray diffraction analyses revealed residual crystalline As and Se in a glass matrix. The material also contained porosity. It was concluded that the level of effort required to upgrade the quality of this material to required levels was roughly equivalent to synthesizing the glass from elements.

The material purchased from Unimetrics was in the form of IR cell windows. X-ray diffraction analysis of the material indicated that it was completely amorphous and IR spectrographic analysis of the bulk material was confirmed by measuring the absorption coefficients exhibited by unclad hand drawn fibers. This material was found adequate from all considerations and was selected for subsequent fiber drawing experiments.

2. Feed Preparation

All of the As_2Se_3 material purchased from Unimetrics was homogenized by melting to insure that the refractive index was uniform and to provide a fixed reference from which the refractive index of the core glass was adjusted. The homogenization was felt necessary because the As_2Se_3 cell windows were reportedly made by a vapor phase growth process so AS/Se ratio variations could be anticipated between different windows as well as within individual windows. The index of refraction is quite sensitive to the As/Se ratio. Melting was done in quartz ampoules.

The quartz ampoules were cleaned, filled and evacuated by conventional procedures. Cleaning consisted of soaking in a standard reagent grade glass cleaning solution (35 cc saturated sodium dichromate in 1 liter concentrated sulfuric acid) followed by distilled water and

methanol rinses. The As_2Se_3 glass was degreased in xylene and methanol prior to breaking it up into chunks in a polyethylene bag. These glass chunks were placed in the ampoule with polyethylene tweezers as quickly as possible to minimize exposure. The ampoule was sealed off after evacuation to a pressure of 2×10^{-5} torr.

The glass was homogenized by melting at temperatures between 650 to 700°C. The bulk glass was held at temperature for approximately 5 hours. The core composition, which was made up from a portion of the homogenized bulk glass and an appropriate Te addition, was held at temperature for 68 hours. In both cases, the hot ampoules were shaken periodically to enhance mixing.

The core glass (Sample No. 38-B-1) was prepared by mixing 0.125 grams of Te with 11.162 grams of the previously homogenized bulk glass. The materials handling and melting procedures used for the core glass were the same as those used with the bulk glass. This Te addition was calculated to raise the index of the core glass over that of the cladding glass (Δn) by 0.0173. For this index difference fibers should support only a single optical mode for core diameters less than approximately 25 microns and two modes for diameters less than approximately 60 microns.

Doped core glass samples were analyzed by an X-ray microprobe technique (EDAX) to insure that the Te was distributed uniformly in the glass. Samples which had been subjected to the 700°C - 68 hour melting cycle were uniform. Other samples which had been melted for shorter times at lower temperatures exhibited heterogeneities.

3. Fiber Drawing

The drawing process consisted of charging the reservoirs with glasses, heating them to the drawing temperature and pulling the fibers after initiation.

After cleaning and assembly, the reservoirs were filled with broken pieces of the previously melted core and cladding glasses. The glasses were broken and cleaned by the same procedures used to homogenize the glasses. Large diameter pieces of glass were used to fill the reservoirs to minimize the surface to volume ratio; and, thus, the problems

of contamination and fining. A helium gas flow was initiated through the glass reservoirs prior to heating.

Assembled and charged glass reservoirs were then inserted into the vertical furnace and heated to the fiber drawing temperature. The furnace was preheated in some cases. Preheating did not effect the process or quality of the drawn fibers other than reducing the time between charging and drawing. Diffusive mixing between the two glasses and uncontrolled flow from the tips were prevented by blocking the two orifices. The most expedient procedure was to lower the inner reservoir until it blocked the outer orifice and to block the extended inner orifice with a graphite plug. This blocked condition was maintained during heatup and soaking. Just prior to pulling, the inner reservoir was raised to a predetermined position and the graphite block was removed.

Fiber drawing was initiated by allowing a glob of glass to drop from the concentric tips and in so doing pulling a "transient" fiber. This transient fiber was then attached to the rotating drum with tape and drawing was continued without interruption until a steady state condition was established. Diameters were varied by changing drum speed or orifice position during a fiber drawing run. No temperature changes were made during a fiber drawing run.

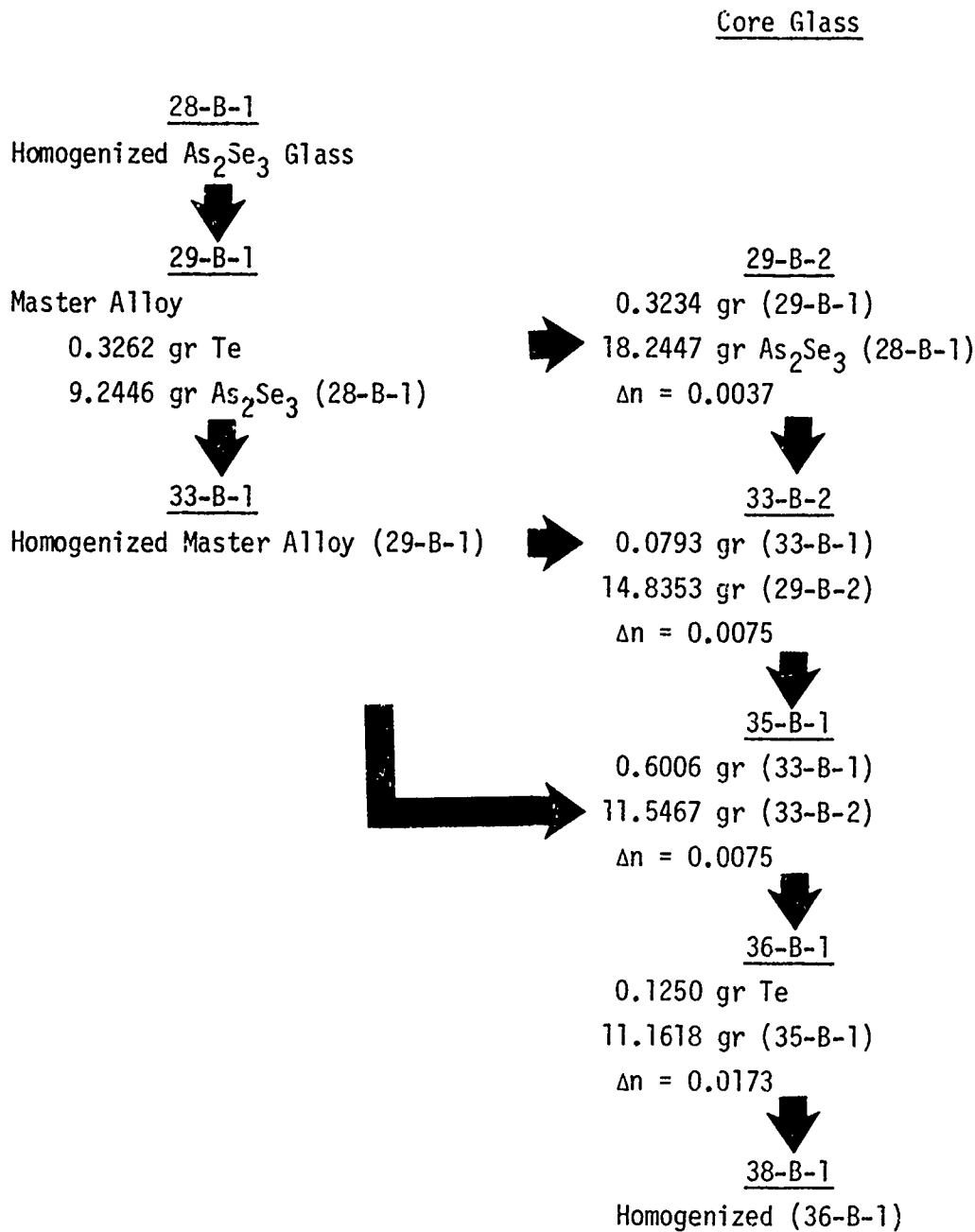
The fiber drawing conditions and dimensional characteristics are summarized in Table I. The calculated index differences between core and cladding are also tabulated. The specific combinations of cores and claddings which were produced as well as processing histories are summarized in Table II.

The index difference between core and cladding was increased progressively during these series of fiber drawing experiments. The lower index differences were selected to maximize permissible core diameters while satisfying the single mode criterion. We were unable to detect the T_e at these concentrations and thus had no direct means of measuring core diameters. The T_e level was gradually increased until it could be detected by X-ray micropobe. The latter fibers were drawn from compositions with a calculated index difference of 0.0173 which should permit transmission of only a single mode for core diameters up to approximately 25 μm .

TABLE I
SUMMARY OF DRAWING CONDITIONS AND PHYSICAL CHARACTERISTICS OF As₂Se₃ GLASS FIBERS

Fiber Designation	Core Designation	Cladding Designation	Calculated Δn	Orifice Position (cm)	Tip Temperature (°C)	Drawing Speed (cm/sec)	Fiber Diameter (cm)	Core Diameter (cm)
31-B-1	29-B-2	As received	.0037	below	312	14.3	.0076	
-2	"	"	"	"	"	19.3	.0046-.0051	
-3	"	"	"	"	"	24.4	.0036	
-4	"	"	"	"	"	14.3	.0041-.0056	
33-B-1	29-B-2	As received	.0037	~.12 below	316	3.2	.033	
-2	"	"	"	"	"	7.2	.0165	
34-B-1	33-B-2	As received	.0075	.05 below	316	4.6	.0168-.0190	
-2	"	"	"	"	"	8.6	.0111-.0091	
-3	"	"	"	~even	"	4.6	.0205	
-4	"	"	"	"	"	8.6	.0122	
-5	"	"	"	"	"	10.0	.0185-.0206	
-6	"	"	"	"	"	12.6	.0122-.0155	
-7	"	"	"	"	"	15.3	.0076-.0127	
37-B-1	33-B-1	As received	.0546	~.1 below	303	2.4	.0228	.0035
37-B-2	33-B-1	As received	"	~.1 below	303	4.6	.0145-.0182	
-A	"	"	"	even	316	2.7	.0145	
-B	"	"	"	"	"	2.8	.0187	
-C	"	"	"	"	"	4.6	.0157-.0170	
-D	"	"	"	"	"	6.6	.0129-.0157	
-E	"	"	"	"	"	8.6	.0094-.0112	
-F	"	"	"	"	"	3.8	.0112	
39-B-A	38-B-1	28-B-1	.0173	~even	316	2.7	.0128	.0025
-B	"	"	"	"	"	2.7	.0107-.0157	.0048
-C	"	"	"	~.1 below	323	2.7	.0091-.0096	
40-B-1	38-B-1	28-B-1	.0173	~.05 below	316	2.4	.0119	.0033
-2	"	"	"	~even	"	2.4	.0104-.0114	
41-B-1	As received	-	-	-	306	2.8	.025	
41-B-2	Homogenized Cladding 28-B-1	-	-	-	306	2.8	.011-.012	
41-B-3	Core Glass 38-B-1	-	-	-	306	2.8	.013	

TABLE II
SUMMARY OF GLASS PROCESS HISTORY



4. Analysis of Fiber Drawing Process

The physical characteristics of the fibers were analyzed to verify that the process functioned as designed.

As indicated previously, the double orifice drawing system was designed to produce fibers up to 150 μm diameter with cores in the range of 25 to 60 μm at growth rates of approximately 10 cm per second from glass melts with viscosities of approximately 1000 poise. Extrapolated kinematic viscosities of As_2Se_3 glass shown in Figure 3 indicate that a 1000 poise viscosity is reached at approximately 325°C. It can be seen from Table I that the drawings speeds, outside diameters and core diameters are generally within the target ranges for glass temperatures in the range of 303 to 316°C. Core diameters ranged from 25 to 47.5 μm and overall diameters from 90 to 225 μm . The agreement between the designed and observed performance indicates that the fiber drawing process is functioning as anticipated and is well controlled.

Fiber drawing theory predicts that, under constant temperature conditions the fiber diameter should vary as $V^{-1/2}$, where V is the drawing speed. The results shown in Figure 4 do not allow one to determine whether this relationship was met over the limited range of drawing speeds investigated; however, there is every reason to expect this to be the case since this relationship has been observed with silicate glasses. (9) There appear to be some anomalies with respect to fiber diameters at nominally identical drawing conditions. These displacements of diameter vs. pulling speed probably result from glass temperature differences since this glass has a very narrow temperature range over which it can be drawn (it is a short glass) and the actual temperature in the tip area is a strong function of the intimacy of the thermal contact between the bottom heater plate and the tip. In the future it would be desirable to extend the drawing speeds over a wider range and to improve the accuracy of the temperature control at the tip. These two procedures would permit better definition of the process as well as improving process control.

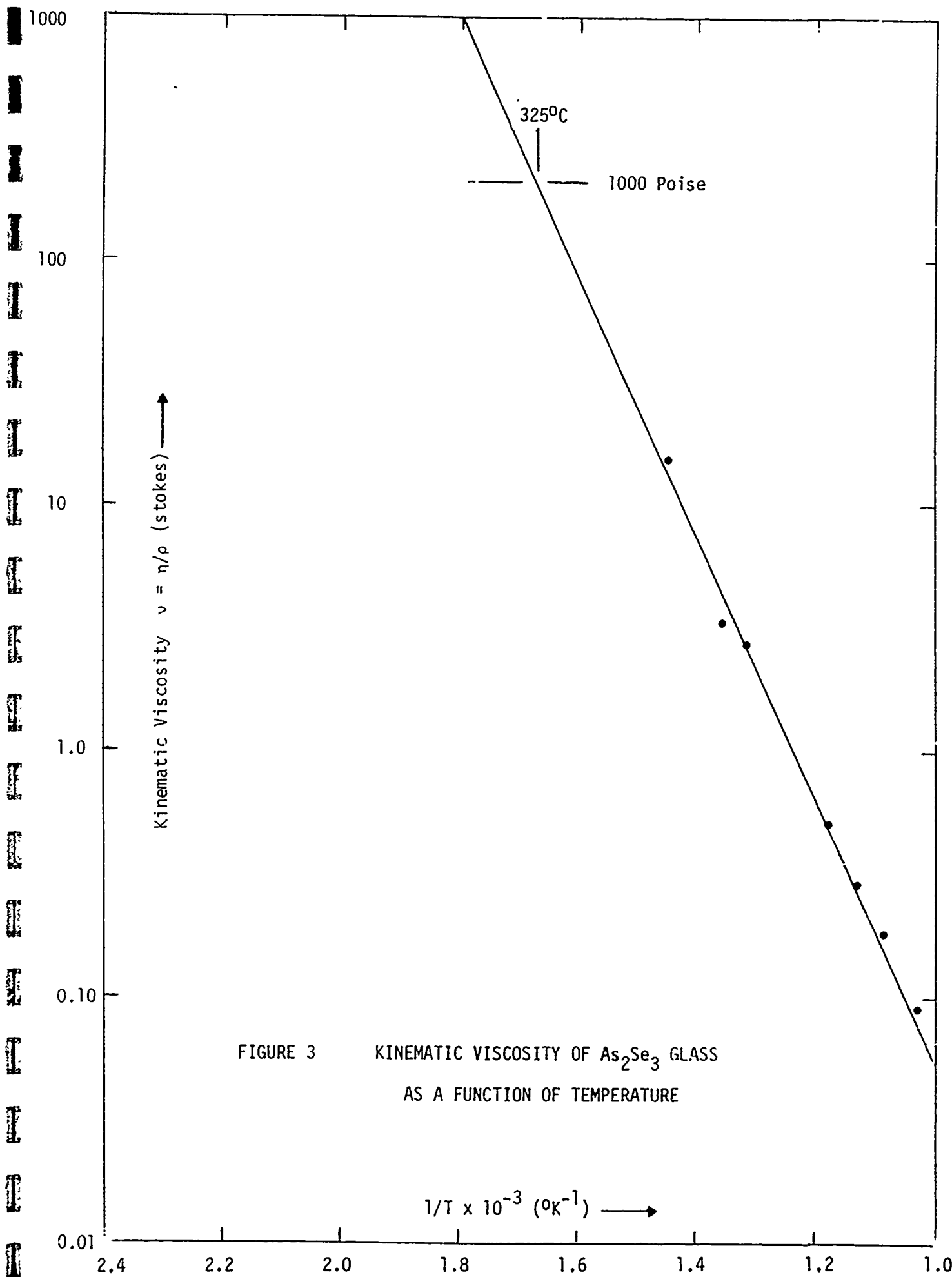


FIGURE 3 KINEMATIC VISCOSITY OF As_2Se_3 GLASS
 AS A FUNCTION OF TEMPERATURE

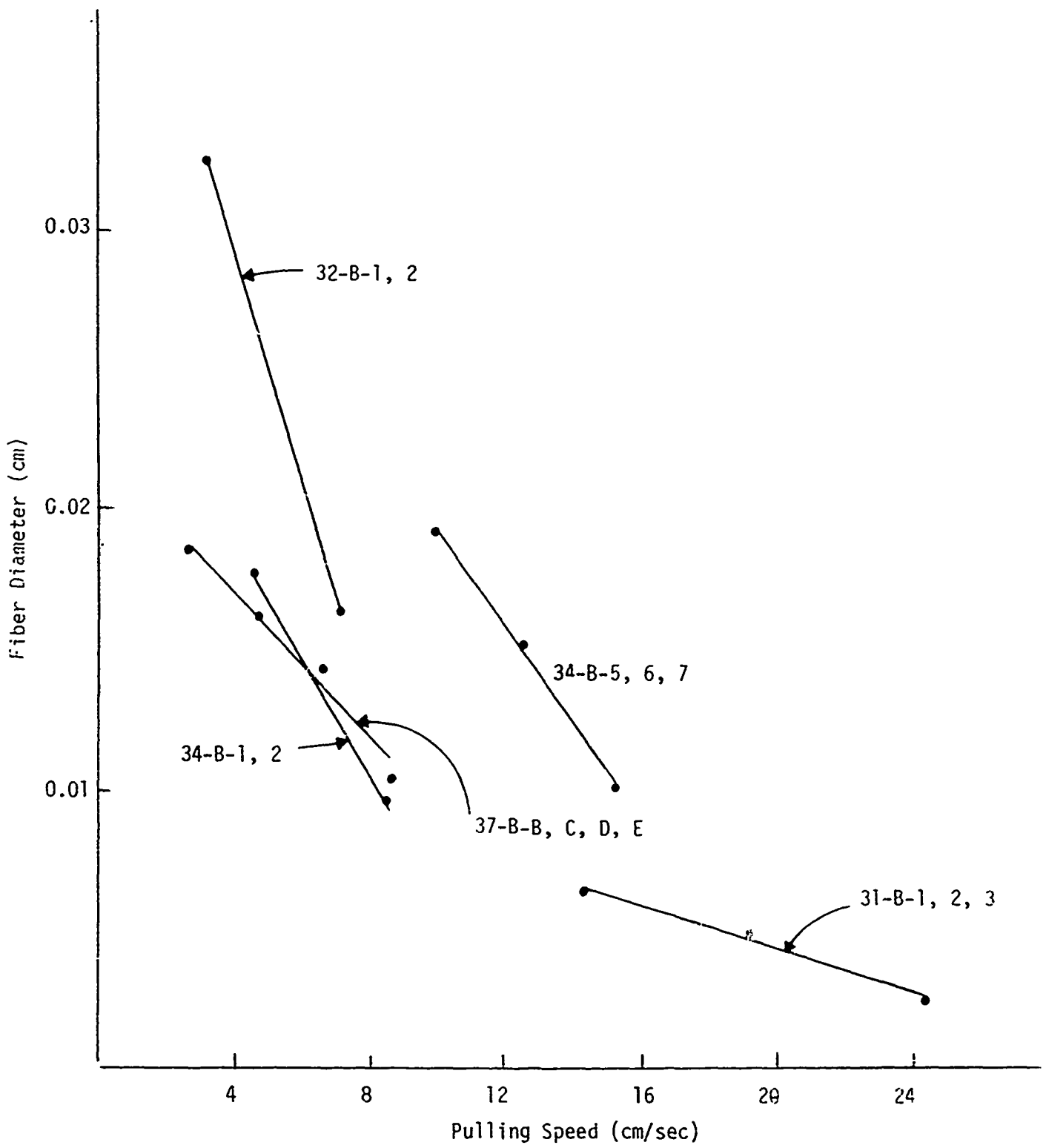


FIGURE 4 FIBER DIAMETER VS. PULLING SPEED

Several fiber drawing runs were made from the concentric orifice tips with As_2S_3 glass used as a cladding and As_2Se_3 used as a core. The As_2S_3 glass is transparent in the visible spectrum which permitted the geometry of the core and cladding to be observed directly. This materials combination was not an ideal model system since the sulfide glass has a higher viscosity than the selenide glass in the drawing temperature range. It was also not an appropriate combination for 10.6 μ m optical wave guides because the sulfide glass has a relatively high absorptivity at this wave length. Despite these deficiencies, these drawing experiments did permit observations to be made about the core/cladding diameter ratio, the core shape and size uniformity and its concentricity within the cladding. These types of observations are extremely difficult to make by X-ray micro-probe techniques which were required for the doped selenide glass fibers.

Metallographic sections of these model fibers showed that the cores were well centered in the cladding. In general, the shape of the cores were distorted from a circular cross section. The difference between the major and minor diameters of the nominally elliptical cross sections were in the range of 5 to 14%. In contrast, the outside shapes were circular and diameter uniformity was generally within 2% under steady state pulling conditions. It is probable that the noncircular cross sections of the cores resulted from the mismatch in viscosities in this model system. If there is a mismatch between the viscosities of the core and cladding glasses, it is better to work with materials combinations that yield a core glass with a higher viscosity than the cladding glass⁽⁴⁾ in contrast to the glasses used in these experiments. These modeling experiments also showed that core and cladding diameters could be achieved that were within the desired ranges. Nominal inner orifice positions were established for the doped selenide glass drawing experiments with these model experiments using the sulfide-selenide glass combination.

With the exception of the noncircular core cross section, these model fiber drawing experiments showed that the process was well controlled and yielded useful processing information for the doped selenide fibers. It is expected that cores in the doped selenide glasses should be more nearly circular since the viscosities of the core and cladding glasses are matched. This conclusion follows the characteristics of silicate glass fibers drawn from concentric orifice bushings.

Physical characterization of the Te doped selenide glass fibers consisted of core diameter determination and measurement of external dimensions of fibers. Core diameters were determined by using an X-ray microprobe technique to locate and measure the dimensions of the regions which contained the Te dopant. Approximately 250 Å diameter spots were analyzed on 5 μm spacings in this characterization procedure. The core diameter was measured in one direction after the center of the fiber had been located and then was measured in the orthogonal direction by rotating the sample 90°. Two factors prevent definitive conclusions to be made regarding the shape and dimensional uniformity of the cores. The low signal to noise ratio between the Te L_α and L_β peaks and the background did not always give a clear distinction between the core and cladding regions. Secondly, the 5 μm spacing between analyzed spots sets the precision limit of the diameter determination. With these two limitations, it appears reasonable to place tolerance limit on the observed core diameters and of their uniformity equal to $\pm 5 \mu\text{m}$. It is believed that the cores are substantially more uniform than this tolerance would suggest.

IV. OPTICAL CHARACTERIZATION

Fibers drawn during this program were characterized optically by a technique that was intended primarily as a means of evaluating the drawing process in terms of optical absorptivity for 10.6 μm radiation. It was not intended that the details of the transmitted mode structure would be evaluated. The apparatus, the results of optical characterization and sample preparation procedures are described below.

A. Sample Preparation

Single crystal fibers and early glass fibers were finished by mounting and polishing followed by removing fibers from the mounts. This technique was extremely time consuming and frequently resulted in rounded ends on the fibers. It was found that the surfaces resulting from fracturing diamond scribed glass fibers were usually smooth and nearly perpendicular to the fiber axes. There was generally negligible surface damage from the scribing process. The individual ends could be examined quickly and reformed until adequate quality ends resulted. The scribe and fracture technique was used with all measurements reported in this work.

B. Apparatus for Optical Attenuation Measurements

Attenuation coefficients were determined with the apparatus shown schematically in Figure 5. Chopped radiation is focused onto the fibers. Exiting radiation is collected with a spherical reflector which in turn focuses it onto a detector which measures its intensity utilizing a phase lock amplifier.

The following points describe the specific components in this apparatus:

1. The IR source is a Perkin-Elmer No. 4570244 Mounted Source Assembly which employs a ceramic-coated resistance wire heated to approximately 1100°C.
2. An aperture is used at the exit of the source to minimize the light scattered into the system.
3. The light is modulated at 36.5 Hertz with a mechanical chopping wheel.

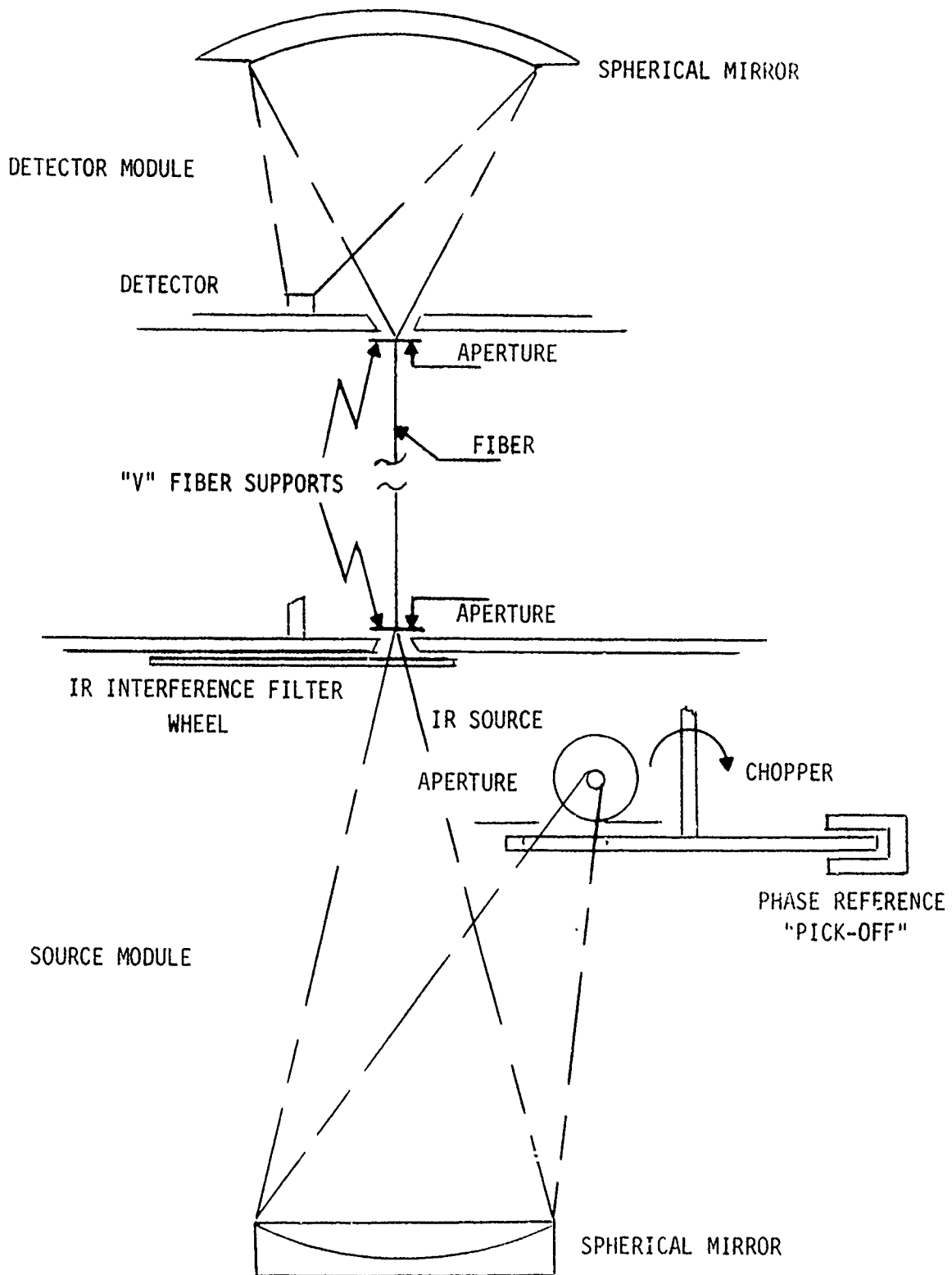


FIGURE 5 SCHEMATIC REPRESENTATION OF APPARATUS UTILIZED FOR OPTICAL ATTENUATION AND NUMERICAL APERTURE MEASUREMENTS

4. A 6-inch diameter, 6-inch focal length mirror is used to focus the emitted radiation onto the entrance end of the fibers. The entrance cone angle is approximately 30°.
5. The wavelength of the incident radiation is defined by filters. Two filters of 0.1 micron bandwidth centered at 3.5 μm and 10.6 μm have been used. An open position is used for alignment.
6. The radiation exiting the fibers is captured by a 6-1/2 inch diameter, 3 inch focal length mirror and focused onto a detector. The acceptance angle of the detector module is approximately 55°.
7. A relatively large pyroelectric detector (2 mm square) is used to compensate for aberrations caused by operating the sphere off axis as well as misalignment.
8. The signal from the detector is measured with a phase-lock amplifier whose reference is set by an optical "pick-off" on the chopper wheel.
9. The fibers are supported at each end by "V" shaped jigs.

C. Attenuation Coefficient

The attenuation coefficient is determined by measuring the light transmitted through the fibers as a function of length and least square curve fitting the resulting transmissions. In this work, transmission for a series of fibers of varying lengths and cross sectional areas were measured. In a second step, the fiber was removed and detector and source modules brought near each other so that the detector and source images coincided. The signal transmitted without a fiber was measured. Under the assumptions that the source image filled both the fiber face in the first and the detector in the second measurement and that the solid angles were equal, a relative transmission (T_R) was defined:

$$T_R = \frac{S_f/A_f}{S_{w/o}/A_d}$$

- T_R = Relative transmission
- S_f = Signal transmitted through fiber (mV)
- A_f = Area of Fiber (cm^2)
- $S_{w/o}$ = Signal transmitted without fiber (mV)
- A_d = Effective area of the detector (cm^2)

The attenuation coefficient is determined from the slope of a line representing the relative transmission versus fiber length on a semi-log plot.

D. Results of Optical Attenuation Measurements

Representative attenuation measurements are plotted in Figure 6.

The histories of these fibers are:

- As received - unclad fiber pulled from sawed bars
- 41-B-1 - unclad fiber pulled from as received material but crushed prior to drawing
- 41-B-2 - unclad fiber pulled from homogenized as received glass which was crushed prior to drawing
- 41-B-3 - unclad fiber pulled from core glass composition which had been Te doped, homogenized and crushed prior to drawing.
- 39-B-B } - clad fibers designed to transmit a single mode
- 39-B-C }
- 40-B-1 }

Approximately an order of magnitude increase in the absorption coefficient was observed for the cladding-glass composition after crushing compared with the absorption coefficient of fibers pulled from uncrushed glass. Homogenization did not effect the absorption coefficient of this glass significantly beyond the effect of crushing. The Te doped core glass exhibited an absorption coefficient which was approximately still another order of magnitude higher. It is apparent that the bulk absorptivity of the As_2Se_3 glass was adversely effected by the materials handling procedures. Degradation resulting from the crushing steps appear to have been more significant than the homogenization steps. Possible reasons for the degradation and the characterization techniques which were used to identify the absorption mechanism are discussed later. The absorption coefficients of the clad glass fibers were intermediate between the bulk

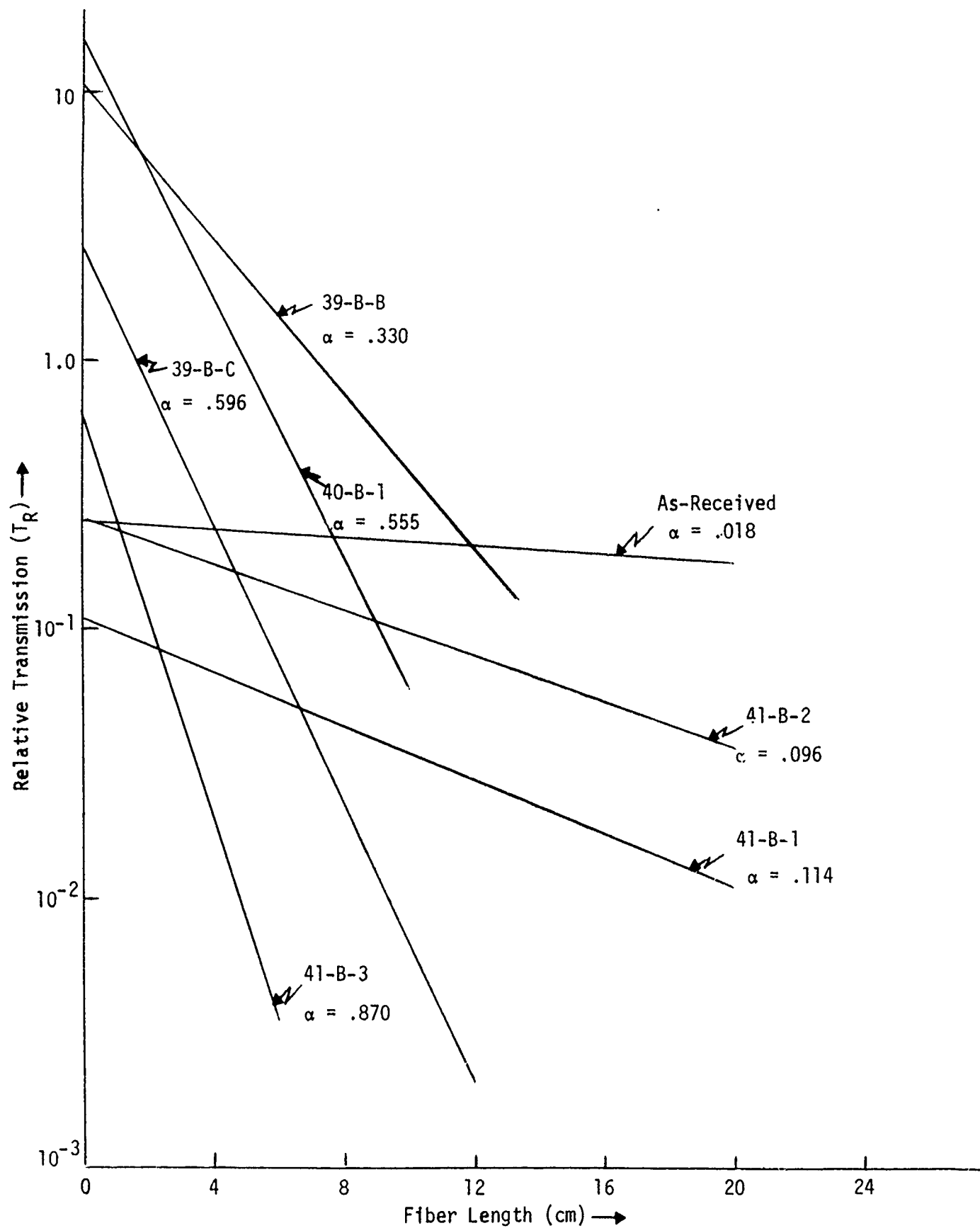


FIGURE 6 REPRESENTATIVE RELATIVE TRANSMISSION MEASUREMENTS. FIBER DESIGNATIONS AND CALCULATED ABSORPTION COEFFICIENTS ARE SHOWN

absorptivities of the homogenized core and cladding glasses.

The intercepts of the relative transmission curves at zero length reveal a difference in behavior between the clad and unclad glass fibers. For an unclad fiber, the intercept should equal approximately the net transmission through two partially reflective surfaces due to Frisnel reflection losses. For As_2Se_3 , the transmission without absorption should be 62% or 65% if multiple internal reflections are included. The average of the four unclad fiber intercepts is 34% which is within a factor of two of the theoretical value. The highest observed intercept equals the theoretical value. It should be expected that the observed intercept will be lower than the theoretical value because the scribed and fractured entering surfaces of the glass fibers were not perfect; thus, the total beam impinging on the surface was not launched into the fiber. The intercepts observed for the clad fibers are all greater than unity when calculated on the basis of core area. It is felt that this is a clear indication that cladding modes were launched in these fibers and that the observed absorption coefficient represents a combination of the attenuation of cladding and core launched modes. Qualitatively it seems plausible that these absorption coefficients should be intermediate between the bulk absorptivities of the core and cladding glasses.

Plastic coatings which were highly absorbing at $10.6 \mu m$ were used in an attempt to strip the cladding modes from the clad fibers. These coatings had refractive indices which were lower than those of the glass fibers. Surprisingly, the plastic coated fibers exhibited lower absorptivities despite the high absorptivity of the coatings. We were not able to deposit higher index mode stripping coatings within the financial and time constraints of the contract. A vapor deposition technique would probably have been required since the melting points of all appropriate materials which were identified were higher than the glass fibers could survive.

Attenuation measurements were also made on selected fibers as a function of the core angle of the incident light. These measurements were made as a means of distinguishing between losses due to bulk absorption within the glass fibers and those caused by losses at the core-cladding interface.

The measurements were made by blocking the central section of the source mirror with disks of successively increasing diameters. Transmission values for concentric annulus around the fiber axis were then determined by subtracting successive measurements. The angle included in each annulus was 2 to 3°. A relative transmission value was then determined for each annulus as follows:

$$T_{R,\theta} = \Delta S_{\theta,f} / \Delta S_{\theta, w/o}$$

$$T_{R,\theta} = \text{Relative transmission}$$

$$\Delta S_{\theta,f} = \text{Signal for cone } \Delta\theta_i \text{ with fiber (mv)}$$

$$\Delta S_{\theta, w/o} = \text{Signal for cone } \Delta\theta_i \text{ without fiber (mv)}$$

The relative transmission values for each fiber were then normalized to the largest relative transmission value.

The normalized $T_{R,\theta}$ data for several fibers is plotted as a function of the annular cone angle in Figure 7 for an unclad fiber 41-B-1 and two lengths of the clad fiber 39-B-C. The annular cone angles plotted correspond to the weighted centers of the 2-3° annuli. Half of the cone area lies on either side of the cited angle. Plotted data runs from zero to 12° which is the practical limit for measurements with the apparatus employed.

These results show that the transmitted light decreases with increasing length and with very strongly increasing angle of incidence. Both results suggest that interface losses are dominant.⁽⁴⁾ If it is assumed that the majority of the light transmitted in the clad fibers is transmitted by way of cladding modes, then a comparison between the clad and unclad fibers indicates that the rate of transmission loss increases with reduced diameter. This is also consistent with interface losses being the dominant loss mechanism--but at the fiber-air interface rather than the core-cladding interface. Based on the results of the total transmission measurements discussed above, it is believed that this is, in fact, what was observed in these measurements.

The lengths of the clad fiber exhibited an essentially constant transmission with increasing angle of incidence beyond 6-7°. It is suspected that this light was transmitted by way of the cores. The theoretical numerical aperture of these fibers ($n = 2.7$, $\Delta n = 0.0173$) is 17.8°, so

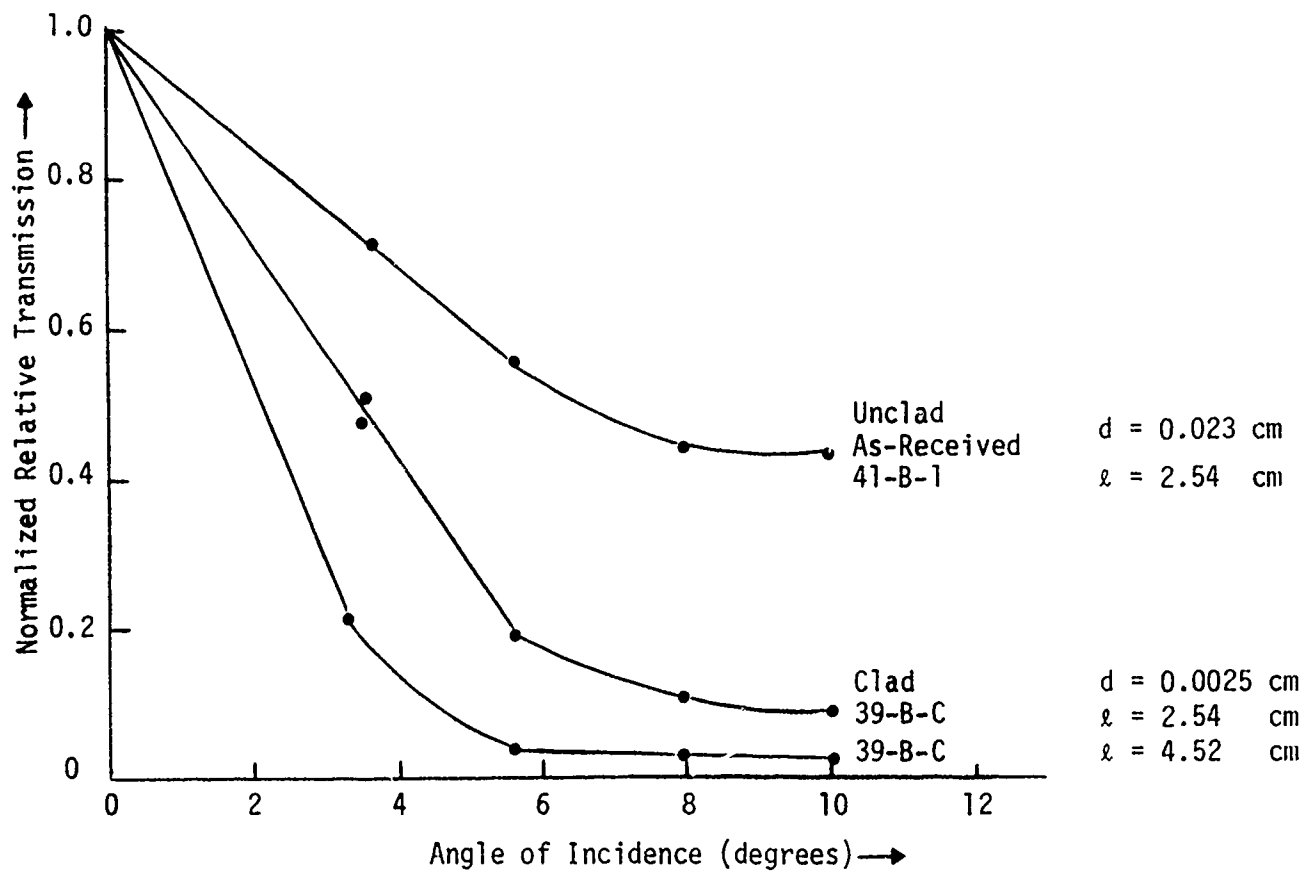


FIGURE 7 NORMALIZED RELATIVE TRANSMISSION ($T_{R,G}$) AS A FUNCTION OF ANNULAR CONE ANGLE

rays beyond 6-7° should have been accepted readily. Also, the difference in the signals transmitted through the 2.54 and 4.52 cm long fibers agrees closely with that predicted on the basis of the absorptivity measured for the core glass. We have no explanation for an indication of a similar effect in the unclad fiber.

The increase in absorptivity that was observed after crushing the glass could have resulted for several reasons. These include an increased bulk absorptivity, the presence of heterogeneities in the bulk or on the surface which act as local absorption sites or scattering sites. The heterogeneities can include such things as crystallites resulting from devitrification, impurities, incompletely dissolved Te and voids. It is apparent that crushing the glass exposed surfaces to air and other contaminants which ultimately become part of the bulk glass after remelting. Also, the glass had to be melted in a manner which would permit the entrapped voids to be eliminated from the molten glass before it was drawn into fibers. It was believed that the handling techniques which were employed would have eliminated these defects; however, it is apparent from the results that this was not the case. Several fibers were examined to attempt identification of the dominant defect.

X-ray diffraction analyses of fibers were made to determine whether devitrification products or other crystalline contaminants were present in the fibers. No evidence was found for the presence of crystalline phases. These results indicate that if a crystalline phase were present, its concentration was less than 1%.

Fibers from all stages of processing were subjected to microstructural analysis by optical and scanning electron microscopy. All of the fibers were free of microstructural defects except the unclad fibers drawn from the core glass composition. These fibers contained widely dispersed particles on their surfaces which were found to contain Si by X-ray microprobe analysis. It appears that particles of the fused silica ampules were incorporated into the sample of Te doped As_2Se_3 glass from which the fibers were drawn. No similar particles were found within the clad fibers so it appears that the remainder of the doped core glass was free of this contamination. It should be pointed out that the probability of inter-

cepting a widely dispersed heterogeneity in any specific section through a fiber is low, so the conclusion about the other clad fibers being free of this defect should not be accepted without further work. However, the absorptivities of unclad fibers drawn from the crushed cladding glass composition exhibited an increased absorptivity and did not have these particles on their surfaces. Thus, the particles were probably not responsible for the dominant absorption mechanism. There was no evidence of voids in the fibers; thus, the melting procedure prior to drawing permitted the voids entrapped between the crushed feed glasses to migrate out.

Optical absorptivities of selected fibers were measured at 3.5 and 10.6 μm . It was anticipated that bulk absorption or scattering loss mechanism should exhibit a wavelength dependence. In all cases the absorptivities at the two wavelengths were essentially identical.

These characterization techniques of the glass fibers did not give any clear indication of the mechanism responsible for the increased absorptivity that followed crushing the glass. It is probable that better fibers can be made by employing casting or extrusion techniques to shape the feed materials since there is no evidence that melting was responsible for the increased absorptivity. Further characterization of the fibers and bulk material formed from the crushed glass can be expected to reveal the dominant defect and thus guide improved handling procedures. It appears reasonable to conclude that there is no intrinsic reason why low absorptivity fibers cannot be drawn from these glasses once suitable procedures are defined.

V. CONCLUSIONS

During this phase of the program, it has been demonstrated that As_2Se_3 glass fibers can be drawn by techniques which are well understood and are controllable. It has also been demonstrated that low loss optical wave guides can be drawn from As_2Se_3 glass; however, intermediate materials handling procedures will require further development to avoid degradation of the glass. Resolution of this issue will also require further materials characterization to identify the induced absorption mechanism. Overall, the problems associated with drawing these optical wave guides were more difficult than anticipated but no evidence was found that drawing of low loss optical wave guides for $10.6 \mu\text{m}$ light cannot be accomplished with straightforward materials research.

VI. REFERENCES

- 1) D. Gloge, App. Opt. 10, 2252 (1971).
- 2) Handbuch, der Physik, XIV, p. 369.
- 3) R.D. Maurer, Proc. IEEE, 61, 452 (1973).
- 4) N.S. Kapany "Fiber Optics, Principles and Applications", Academic Press, N.Y. (1967), p. xvi.
- 5) M. Maklad, et al, "Infrared Transmission in Chalcogenide Glasses," Third Conference on High Powered Laser Window Materials, Nov. 12-14, 1973, Vol. 1, Optical Properties, Feb. 14, 1974, Ed. by C.A. Pitha and B. Bendon, p. 69.
- 6) A.R. Hilton, The Glass Industry, October (1967) p. 550.
- 7) B.T. Kobomiets and B.V. Panlor, Optics and Spectroscopy, 22, 149 (1967).
- 8) K.L. Lowenstein, "The Manufacturing Technology of Continuous Glass Fibers" Elsevier Scientific Publishing Co., N.Y. (1973) p. 69.
- 9) W.F. Thomas, "Physics and Chemistry of Glasses", 1, 4 (1960).